

## Werk

**Jahr:** 1980

**Kollektion:** fid.geo

**Signatur:** 8 Z NAT 2148:47

**Digitalisiert:** Niedersächsische Staats- und Universitätsbibliothek Göttingen

**Werk Id:** PPN1015067948\_0047

**PURL:** [http://resolver.sub.uni-goettingen.de/purl?PPN1015067948\\_0047](http://resolver.sub.uni-goettingen.de/purl?PPN1015067948_0047)

**LOG Id:** LOG\_0033

**LOG Titel:** Rock stress in an Icelandic thermal area, with implications on stresses in the Oceanic lithosphere

**LOG Typ:** article

## Übergeordnetes Werk

**Werk Id:** PPN1015067948

**PURL:** <http://resolver.sub.uni-goettingen.de/purl?PPN1015067948>

**OPAC:** <http://opac.sub.uni-goettingen.de/DB=1/PPN?PPN=1015067948>

## Terms and Conditions

The Goettingen State and University Library provides access to digitized documents strictly for noncommercial educational, research and private purposes and makes no warranty with regard to their use for other purposes. Some of our collections are protected by copyright. Publication and/or broadcast in any form (including electronic) requires prior written permission from the Goettingen State- and University Library.

Each copy of any part of this document must contain these Terms and Conditions. With the usage of the library's online system to access or download a digitized document you accept the Terms and Conditions.

Reproductions of material on the web site may not be made for or donated to other repositories, nor may be further reproduced without written permission from the Goettingen State- and University Library.

For reproduction requests and permissions, please contact us. If citing materials, please give proper attribution of the source.

## Contact

Niedersächsische Staats- und Universitätsbibliothek Göttingen  
Georg-August-Universität Göttingen  
Platz der Göttinger Sieben 1  
37073 Göttingen  
Germany  
Email: [gdz@sub.uni-goettingen.de](mailto:gdz@sub.uni-goettingen.de)

## Rock Stress in an Icelandic Thermal Area, With Implications on Stresses in the Oceanic Lithosphere

B. Voight<sup>1</sup>, R. Simon<sup>1</sup>, T. Thorsteinsson<sup>2</sup>, G. Pálmason<sup>2</sup>, C. Taylor<sup>3</sup>, S.H. Seret Opzoomer-Talma<sup>4</sup>, and B.C. Haimson<sup>5</sup>

<sup>1</sup> College of Earth and Mineral Sciences, The Pennsylvania State University, University Park, Pennsylvania 16802, USA

<sup>2</sup> National Energy Authority, Reykjavik, Iceland

<sup>3</sup> 1118 The Colony, Hartsdale, New York, USA

<sup>4</sup> Oranjewoud 625, 8443 G.A. Heerenveen, The Netherlands

<sup>5</sup> University of Wisconsin, Madison, Wisconsin, USA

**Abstract.** Numerical model analysis of the Reykjavik thermal area in southwest Iceland suggests the possibility of a complex regional stress pattern strongly influenced by thermoelastic effects. The thermal areas are predicted to be domains of relatively high compression, surrounded by zones of approximately radially-diminishing compression and circumferential extension. Model results are compared to data from hydrofracture measurements in southwest Iceland by Haimson and Voight (1977), which suggested a direction of maximum horizontal compression roughly normal to the nearby axial rift zone. Though this regional trend seems supported by additional studies, finite element results presented here suggest that the Reykjavik hydrofracture borehole locations may have been influenced by locally-developed thermoelastic stresses. Predicted stresses and stress orientations for measurement sites are in rather good accord with field measurements. A mechanism for 'locking in' thermoelastic strains and associated stresses is postulated, whereby mineralization in open (thermal) fractures in hot rock prevents these fractures from closing once thermal loading is removed. Old thermal areas may therefore still contain residual stresses on the order of  $10^2$  bar which reflect paleotemperature fields. Finally, it is asserted that stresses through the upper part of the entire oceanic lithosphere may be dominated by residual, mainly thermal components. If so, intraplate stresses cannot be simply calculated from plate tectonic forces acting on the boundaries of lithosphere plates.

**Key words:** Iceland – Thermal stress – Residual stress – Plate tectonics – Geothermal – Finite element – Hydrofracturing – Mid-Atlantic Ridge – Ocean lithosphere – Tectonics.

### Introduction

Hydrofracturing stress measurements were recently carried out to about 0.4-km depth in two boreholes in Quaternary volcanic rocks in Reykjavik, Iceland, on the flank of the Reykjanes-Langjökull continuation of the Mid-Atlantic Ridge (Figs. 1 and 2, Haimson and Voight, 1977). The measurements indicated for the borehole sites an orientation of  $\sigma_{Hmax}$  approximately perpendicular to the axial rift zone; this orientation contrasts with stress orientation postulated for fissures, high angle faults, and focal mechanism solutions for earthquakes within the nearby axial rift zone of the Reykjanes Peninsula (Haimson and Voight, 1977, cf. Klein et al., 1973, 1977).

Several interpretations were offered as possible explanations of the data. Among these was the following (Haimson and Voight,

1977, p. 172): '...the possibility of a thermoelastic effect must be raised. It indeed seems likely that a lithospheric plate containing inclusions of abnormally hot rock masses will display an inhomogeneous stress pattern due to the thermoelastic effect (cf. Voight and St. Pierre, 1974). These thermoelastic stresses must be superimposed upon the regional stress field, and their total effect would depend upon the relative magnitudes of each component.

As a highly idealized (plane stress) example we consider here a cylindrical hot inclusion of radius  $a$  and uniform temperature  $T_o$  in an otherwise cold, unstressed plate. The solution is:

$$\sigma_r = \sigma_\theta = +1/2E\alpha T_o, \sigma_{r\theta} = 0, r < a,$$

$$\sigma_r = -\sigma_\theta = +1/2E\alpha T_o (a^2/r^2), \sigma_{r\theta} = 0, r > a.$$

As a general property of such stress states there is assumed a stress discontinuity across the inclusion surface. Letting  $E = 5 \times 10^5$  bar (cf. Table 1),  $\alpha = 8 \times 10^{-6} \text{ }^\circ\text{C}^{-1}$ , and  $T_o = 100^\circ \text{C}$ , we have a uniform value of  $\sigma_r = \sigma_\theta = 200$  bar (compression), in the inclusion, and variable  $\sigma_r$  (compression) and  $\sigma_\theta$  (tension) in the plates. The latter diminish as  $(1/r)^2$ ; at  $r = a$ ,  $\sigma_r = -\sigma_\theta = 200$  bar, at  $r = 2a$ ,  $\sigma_r = -\sigma_\theta = 50$  bar, and so forth. The mathematical effect is the same, incidentally, if we start with a uniformly hot plate and nonuniformly cool it (inclusion is cooled to a lesser degree); the latter description more adequately fits the thermal history of Icelandic rocks as discussed previously. The result, which must be interpreted in terms of more or less continuous rather than discontinuous stress fields, is that high values of compression might be expected within thermal anomalies, with radial compression and circumferential tension (diminishing rapidly with radial distance) expected beyond them. Stresses due to overburden pressure and initial conditions must be superimposed upon these predicted thermoelastic changes so that absolute tension might not ordinarily be expected, in addition, actual stress changes should be expected to be less, than theoretical estimates because of rock strength limitations.

Interpretation of the field data in terms of this simple model was not straight-forward, in large part because of the necessity of assumed temperature and stress discontinuities at the inclusion boundary. The boundary of the anomaly in the field is simply not that sharp (Fig. 2). On balance the possibility of some thermoelastic stress influence seemed supported by the available evidence, in any event the hypothesis of a local thermoelastic effect could not be safely rejected (Haimson and Voight, 1977, p. 173). In this paper a more elaborate attempt is made to examine questions of thermoelastic stress. The finite element technique (as discussed e.g. by Voight and Samuelson (1969) and many others; see, Gallagher, 1975) was employed.

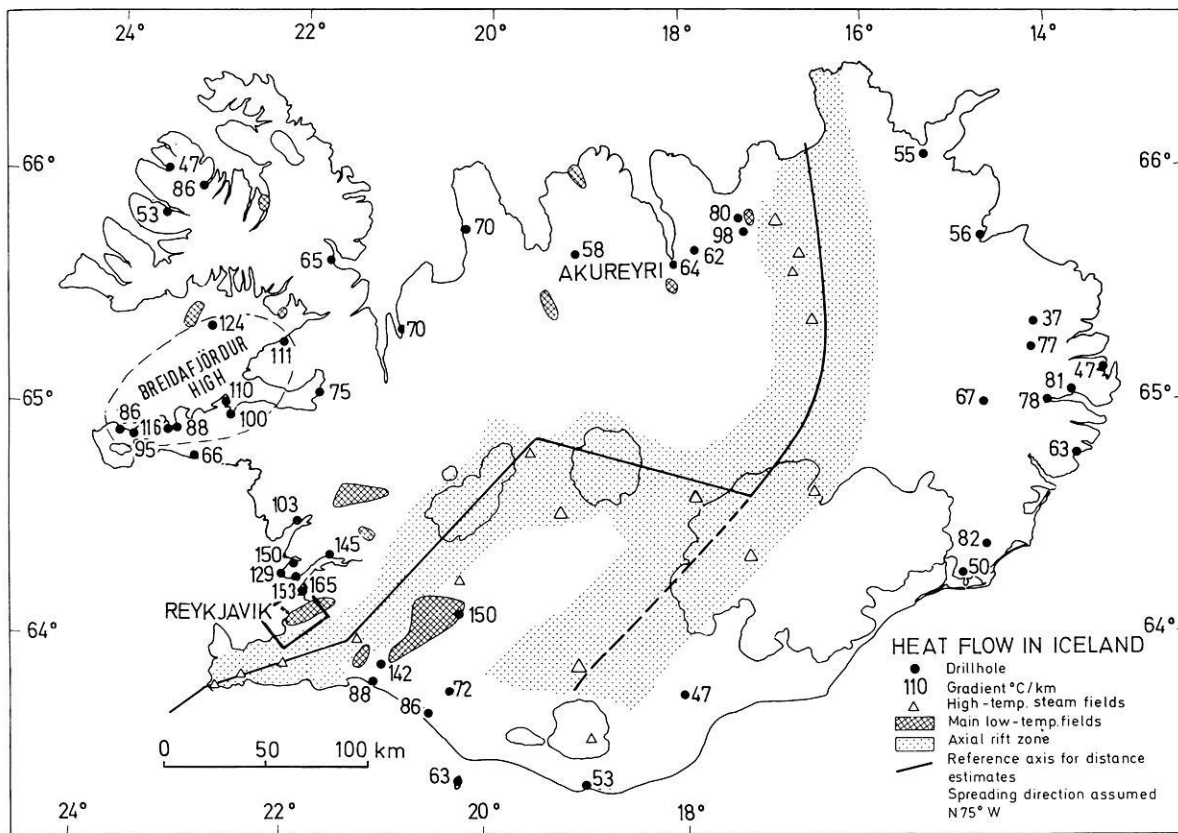


**Fig. 1.** Map of Iceland (after Pálmason and Saemundsson, 1974), indicating regional distribution of surface temperature gradients. Rectangle near Reykjavik represents map area of Fig. 2. The stippled pattern indicates the active zone of rifting and volcanism

### Geometry, Material Properties, Temperature Changes

The area modeled is a rectangle  $24 \times 18 \text{ km}^2$ , with one long boundary at the approximate edge of the axial rift zone (Fig. 1). The Laugarnes hydrothermal system, the site of the hydrofracture measurements, is located approximately in the center of the finite element model. A grid of 186 nodal points (346 plane stress triangular elements) was constructed, with smaller elements in areas of high temperature gradient. Nodal points were located at stress measurement sites. A reference depth of 300 m was selected, inasmuch as many of the borehole measurements cluster about this depth (Haimson and Voight, 1977, Fig. 8).

The rock types of the Reykjavik area include basalt flows in various stages of alteration, interglacial sediments, hyaloclastites, and local dolerite intrusions; the stress measurements were made in basalt and dolerite. Not unexpectedly, therefore, the associated physical properties cover a fair range (Table 1). For most computer experiments the material was regarded as homogeneous, with a Young's modulus of  $4 \times 10^5 \text{ bar}$ , Poisson's ratio of 0.25, and coefficient of linear temperature expansion of  $5.4 \times 10^{-6} \text{ }^\circ\text{C}^{-1}$ . However it is recognized that no single set of elastic constants can accurately describe the field situation. The Young's modulus value at any given point in the rock mass seems correct within a factor of about two with respect to measured laboratory values. A fair correspondence of laboratory and field modulus values is expected because most joints are mineralized at this depth. The other property values were assumed. Alternative approaches would have been to (1) vary element properties within the known range, using for example a random number generator (Su et al.,

**Table 1.** Properties of Rock in Reykjavik Area, Iceland, based on laboratory measurements

Density:	2.4–3.0 Mg/m <sup>3</sup>
Uniaxial compressive strength:	240–2570 bar
Tensile Strength	
Assumed value (1/15 uniaxial compressive strength):	16–170 bar
Laboratory 'hydrofracturing' strength:	21–134 bar
Field 'hydrofracturing' strength:	34–134 bar
Young's modulus:	$1.7\text{--}8.2 \times 10^5 \text{ bar}$

1970), or to (2) specify properties according to the known distribution of specific rock types.

Temperature data were based on the detailed surface thermal gradient map of the Reykjavik area (Fig. 2), showing anomalies associated with Laugarnes, Seltjarnarnes, Ellidaár, and Álftanes thermal fields (Pálmason, 1975). Isolines are given in  $^\circ\text{C}/\text{km}$ , and surface gradients as high as  $500^\circ\text{C}/\text{km}$  are indicated. The surface gradients are not in fact maintained to depths of 1 km and beyond (e.g., Tómasson et al., 1975, Fig. 4), but to 300 m the error in calculated rock temperature seems relatively small, as indicated by drillhole data.

Thermal stresses are due to temperature changes. The simplifying assumption is made that plastic or viscoplastic yielding over geologic time can take place above a given critical temperature,  $T_p$ , but that for rock cooled below this reference temperature the crust behaves essentially elastically. Thermoelastic stresses are

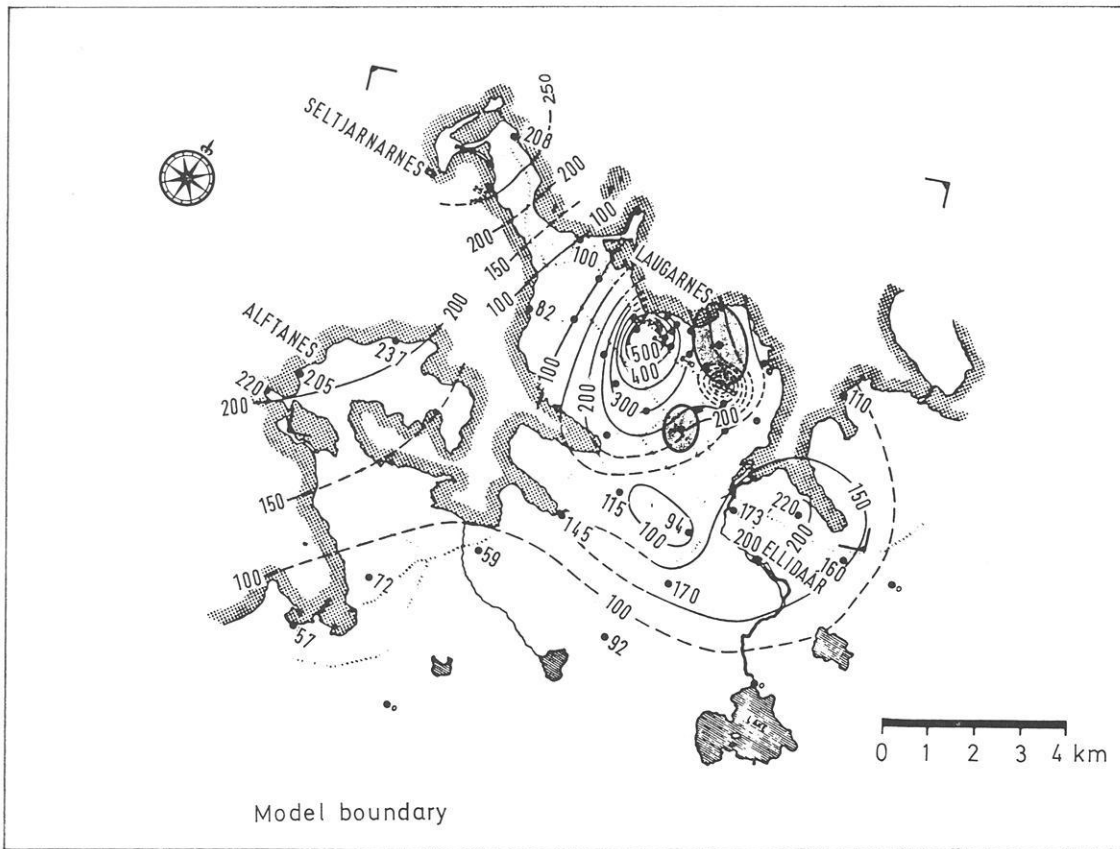


**Fig. 2.** Thermal gradient map of Reykjavik peninsula and adjacent areas (for location see Fig. 1), showing anomalies associated with Laugarnes, Seltjarnarnes, Ellidaar, and Alftanes fields (after Pálmason, 1975). Isotherms in  $^{\circ}\text{C}/\text{km}$ . Stress ellipses noted for boreholes H18 (the larger) and H32, for about 0.3-km depth (after Haimson and Voight, 1977). Water bodies are patterned. Outer rectangle at model boundaries. Four corners show frame of Figs. 3–6

thus limited to  $T < T_p$ . Following Turcotte (1974) we assume  $T_p = 300^{\circ}\text{C}$ . The temperature change for each element was therefore  $T_p - T_{0.3}$ , where  $T_{0.3}$  is the temperature at the 0.3-km level as estimated from the surface gradient at the element centroid.

## Results

If ENE-WSW boundary displacements are restrained (Model I), tensions on the order of 500 bar develop as a consequence of cooling (Fig. 3). The internal stress directions are controlled by the imposed (roller) boundary conditions, with the thermal field variations creating a minor effect. Values of tension are somewhat less (25% or so) over hot spots. The amount of calculated tension is well beyond the tensile strength of the intact rock (by a factor of about 5) and hence also the strength of the rock mass (see e.g. Table 1). Model I therefore is interpreted to predict fracturing of the rock mass more or less perpendicular to the direction of tensile stress, with the principal through-going fractures avoiding the high temperature areas; the tensile stresses would thereby be largely relieved, and the zero-displacement boundary conditions of the original model would be effectively changed to that of boundaries relatively free to displace.

The stresses developed in the model are, of course, proportional to the assumed value of Young's modulus. These stresses could therefore be decreased by assuming a lesser value of Young's modulus. However, because strength and Young's modulus are

not truly independent variables, and because the assumed value of Young's modulus is believed to be of the correct order of magnitude, the broad interpretation of Model I as given above would seem justified.

In the next experiment (Model II), lateral boundaries were assumed unstressed (and free to distort), with internal stress depending solely on the distribution of sustained temperature changes. The pattern in plan view is one of strong biaxial compression within the zone of highest vertical temperature gradients, grading outward to a zone of approximately radial compression and circumferential tension (Fig. 4). Qualitatively similar to the thermal inclusion model discussed in the introduction to this paper, this finite element model more adequately treats the stress changes in terms of complex temperature variations observed in the several thermal areas. Stress measurement data for boreholes H18 and H32 are also plotted as ellipses for comparison with theoretically determined values.

The following information was next considered. The total vertical stress  $\sigma_v$  at a depth of 0.3 km is about  $84 \pm 3$  bar, based on known density of overburden. The measured formation pore fluid pressure at this depth is about 24 bar (Haimson and Voight, 1977, Table 3). Thus the effective vertical stress  $\sigma'_v$  (total vertical stress minus pore fluid pressure) can be taken as 60 bar.<sup>1</sup> If the cohesive

<sup>1</sup> The notation  $\sigma_i$  indicates total stresses; with a 'prime', e.g.,  $\sigma'_i$ , effective stresses are indicated

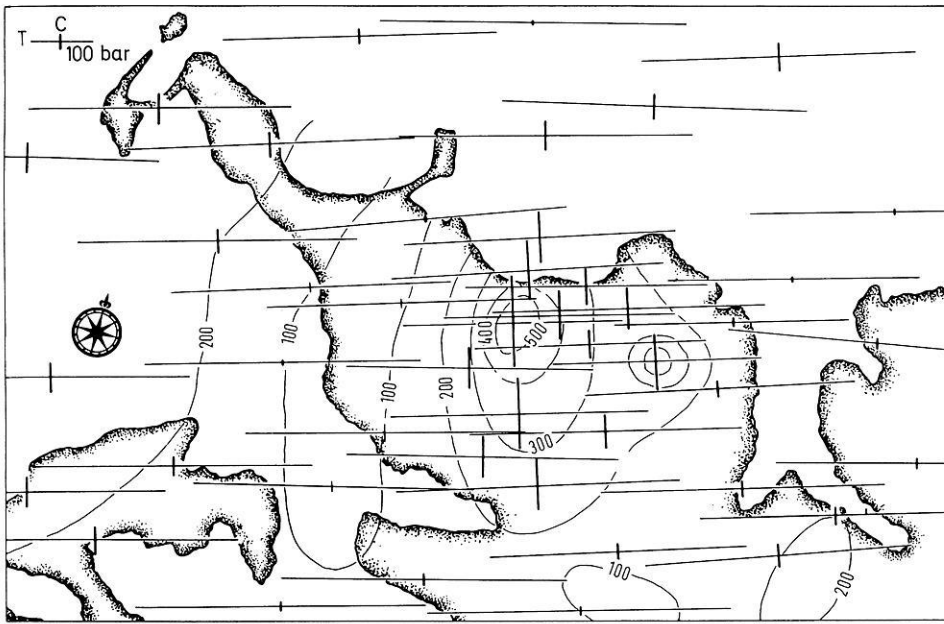


**Fig. 3.** Horizontal effective stress distribution in the Reykjavik peninsula area (compare Fig. 2 for location and scale) at 0.3-km depth. Model I (ENE-WSW motion restrained at boundaries). Stresses are indicated by crosses. Compression (*C*) given by heavy lines, tension (*T*) by thin lines. Stress scale as indicated for tension line in upper left corner. Surface temperature gradient contours are taken from Fig. 2. The model predicts tension fractures roughly normal to the tensile stresses, with the main fracture zones avoiding the domains of highest temperature

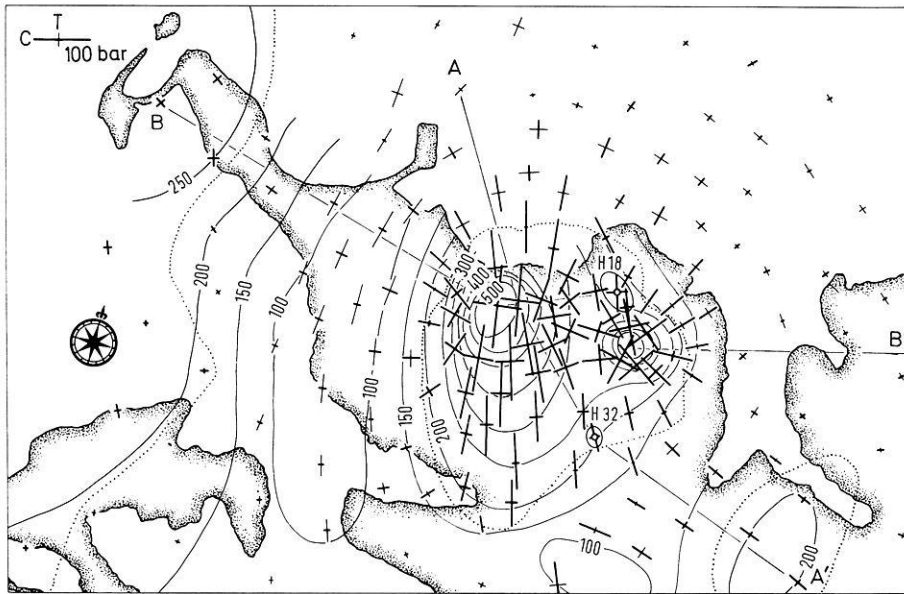


**Fig. 4.** Horizontal effective stress distribution in the Reykjavik peninsula area (cf. Fig. 2 for location and scale) at 0.3-km depth. Model II (freem, unstressed boundaries). Compression (*C*) given by heavy lines, tension (*T*) by thin lines. Stress scale as indicated for compression in upper left corner. Surface temperature gradient contours from Fig. 2. Locations of stress profiles *A-A'*, *B-B'* indicated (cf. Figs. 7 and 8). Measured stress ellipses shown at H18 and H32 sites. Ellipse radii indicate magnitude of compression. Ellipse long axis is direction of  $\sigma_{Hmax}$

resistance is assumed destroyed on marginal faults along the rift zone boundary, the lateral pressure perpendicular to the strike of normal faults at this location (the minimum effective principal stress  $\sigma_3'$ ) is assumed to be given by the product of the effective vertical stress and the term  $\tan^2(45 - \frac{1}{2}\phi)$ , where  $\phi$  = angle of friction, as noted by classical soil mechanics theory. Assuming  $\phi = 30^\circ$ , the effective lateral boundary stress is 20 bar, acting in a northwest direction (if cohesion  $> 0$ ,  $\sigma_3' < 20$  bar). Boundary stresses in the northeast direction are unknown (as indeed are the appropriate limits of the model 'plate'), but at least at the juncture of the northeast edge of the model with the active rift zone faults, these stresses are inferred as  $\geq 20$  bar.

A third model was therefore considered (Model III), consisting of a flat plate, free to deform at boundaries and subjected to

internal thermal loading, with a uniform boundary stress of 20 bar. The solution of Model III is exactly that of Model II (free boundary), except that all principal stress magnitudes are increased by 20 bar. Stress orientations and shear stresses remain unchanged. Therefore, the diagrams of shear stresses and predicted fracture orientations (Figs. 5 and 6) apply exactly to both Models II and III. The diagram of the principal stresses (Fig. 4) is also applicable to both, but for Model III each stress must be increased by a compression of 20 bar. As a result, for Model III a decrease of 20 bar occurs in each of the absolute values of tension indicated in Fig. 4, and a substantial decrease occurs in the area of rock mass subjected to some tensional stress. 'Effective Stress' profiles across the thermal areas are shown in Figs. 7 and 8. The data are for Model II, but the results can be interpreted also for Mo-

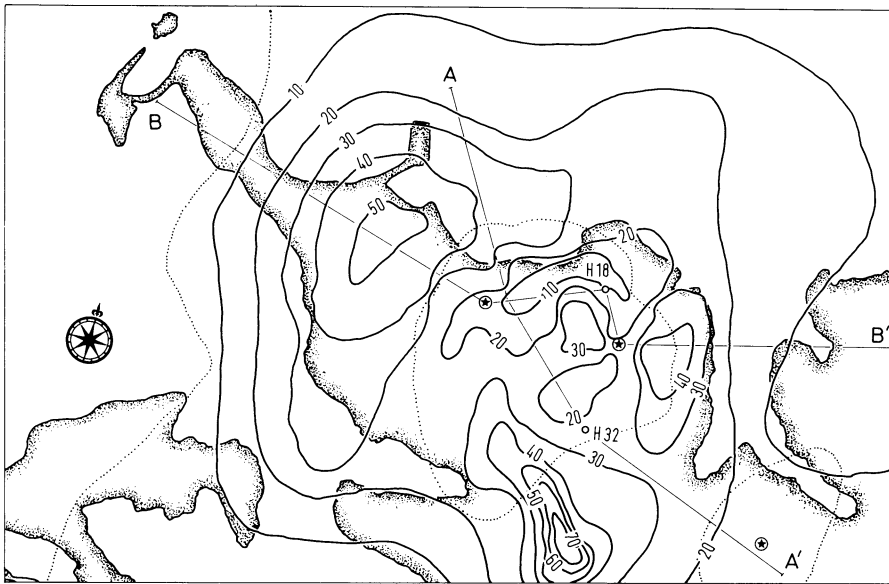


**Fig. 5.** Horizontal shear stress distribution in the Reykjavik peninsula area at 0.3-km depth (cf. Fig. 2 for location and scale). Models II and III. Shear stress isolines are in bars. Locations of stress profile *A-A'*, *B-B'* indicated (cf. Figs. 7 and 8). *Dotted lines* indicate compression-tension boundaries for Model II. *Stars* denote approximate locations of temperature maxima. Stress measurement sites H18 and H32 are shown

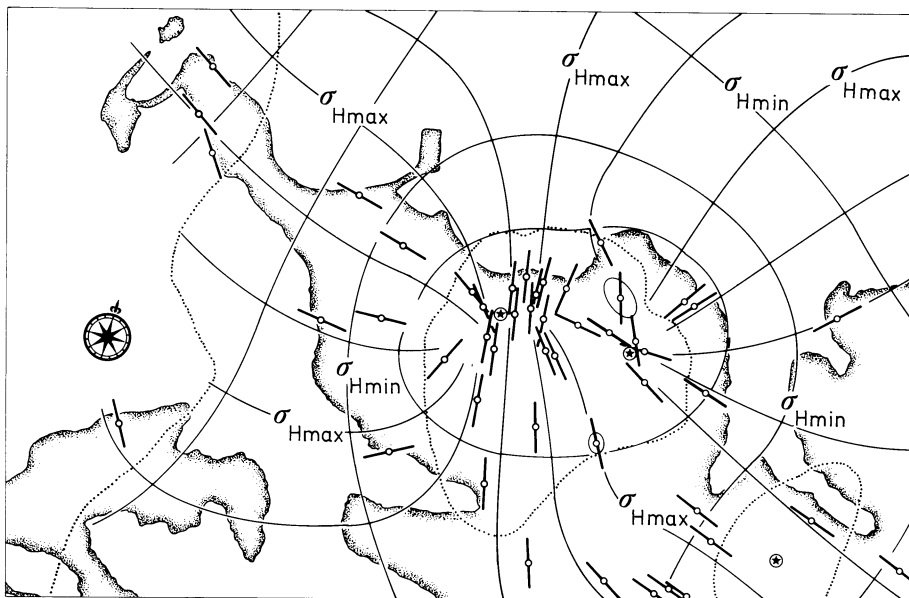


**Fig. 6.** Horizontal stress trajectories of the Reykjavik peninsula area at 0.3-km depth (cf. Fig. 2 for location and scale). Models II and III. Compression reckoned positive (i.e.,  $\sigma_{Hmax}$  is maximum horizontal compression). *Stars*, *dotted lines* as indicated in Fig. 5. Existing boreholes indicated by *circles*, with *heavy lines* denoting predicted extension fracture orientations for the borehole sites. Stress ellipses are indicated for the stress measurement sites. The long axes of these ellipses correspond to observed hydrofracture orientations

del III by superposition of 20 bar on the horizontal stresses. The extent to which the stress profiles mirror the temperature profile is clear.

The effective vertical stress is also indicated on the profiles. It appears that over much of the region at this depth, the predicted vertical stress is the greatest effective principal stress ( $\sigma'_1$ ), compression reckoned positive. Over the hotter parts of the thermal areas, however, the vertical stress becomes the minimum stress ( $\sigma'_3$ ), as the magnitudes of the horizontal stresses become large. Peripheral zones with respect to the hot spots are characterized by  $\sigma'_v = \sigma_2$ .

Hydrofracture stress measurement data for boreholes H18 and H32 are also given in Figs. 4, 6, 8, and Table 2, for comparison with theoretical Models II and III. The correspondence of measured values with results of both numerical models is rather striking, both with respect to stress orientation and magnitude. Indeed, the degree of correspondence seems remarkable in view of the large number of simplifying assumptions required. The fit with

respect to  $\sigma_{Hmin}$  is better than for  $\sigma_{Hmax}$ , but the measured values of  $\sigma_{Hmin}$  are known to a greater degree of reliability due to the nature of the hydrofracturing technique. No 'backfitting' of Young's moduli was attempted, for example, in order to bring measured and calculated stresses into closer correspondence. On the other hand, the observed correspondence does not guarantee the correctness of the assumed elastic properties, for another set of temperature assumptions, on which the stresses also greatly depend, might easily have been employed.<sup>2</sup> No uniqueness of

<sup>2</sup> The 'correct' field value of Young's modulus might be half of that value indicated by laboratory experiments, whereas the assumed critical temperature  $T_p$  might be effectively twice as high. A similar set of predicted stresses might thereby result. The present solution might thus contain an appropriate 'balance' of parametric assumptions even though individual values might be disputed

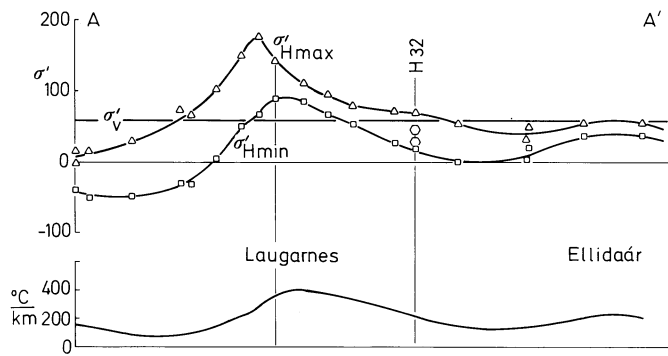


**Fig. 7.** Effective stress and thermal gradient profiles *A–A'*, crossing Laugarnes and Ellidaár thermal domes (see Figs. 4 and 5 for profile location). Model II (for Model III, add 20 bar to indicated horizontal stresses). Stresses in bar, thermal gradients in °C/km. Note excellent correspondence between stresses and thermal gradients. Measured maximum and minimum horizontal stresses at H32 indicated by octagonal symbols. Note change in orientation in principal stresses as a function of position over the Laugarnes thermal high,  $\sigma'_v = \sigma'_3$

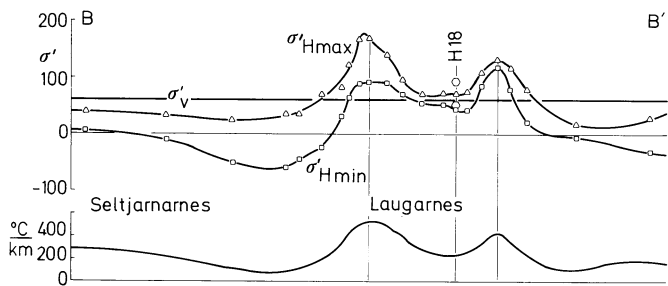


**Fig. 8.** Effective stress and thermal gradient profiles *B–B'*, from Seltjarnarnes through Laugarnes (see Figs. 4 and 5 for profile location). Explanation as in Fig. 7. Measured horizontal stresses at H18 indicated by octagonal symbols

**Table 2.** Comparison of Measured and Predicted Effective Stresses

	$\sigma_{Hmax}$	$\sigma_{Hmin}$	$\tau_{max}$	Direction of $\sigma_{Hmax}$
H18				
Measured	94	50	22	N 45 W
Calculated				
Model II	73	43	15	N 16 W
Model III	93	63	15	N 16 W
H32				
Measured	44	29	8	N 25 W
Calculated				
Model II	71	19	26	N 30 W
Model III	91	39	26	N 30 W

Model II implies zero boundary stress

Model III implies a boundary stress of 20 bars on all sides

All stresses given are effective stresses, i.e., total stress minus pore fluid pressure. Total stresses are as given in Haimson and Voight, 1977, Eqs. (4) and (5), p. 168. Fluid pressure of 24 bar assumed for the 0.3 km level (Haimson and Voight, 1977, Table 3)

solution can therefore be claimed, and it is possible that the close agreement in stresses is largely fortuitous. Nonetheless, the hypothesis that thermal gradients are mainly responsible for the observed rock stresses seems greatly strengthened.

Other experiments were conducted in which alternatively, (1) additional boundary loads were applied, (2) internal fissuring was considered, and (3) local changes in Young's modulus were introduced. Results were as follows:

1. With increased compressive boundary stress along one edge, the stress pattern observed was similar to that of Model III except that the directions of maximum compression were somewhat shifted in the direction of the applied boundary load.

2. Internal fissuring, modeled by local reductions in Young's modulus, caused a general decrease in tensional stresses and a decrease in maximum compression, with a shift of the tension-compression boundary toward the strongly heated area. The overall stress pattern remained similar.

3. In the area of H18 higher modulus rocks (dolerite) are known to occur, and thus a portion of the model was specified with a large value of Young's modulus ( $8 \times 10^5$  bar), all other model aspects remaining the same. Higher values of stresses resulted, as anticipated. The general patterns were similar.

For the moment it seems sufficient to note that each of these factors can exert a modifying effect on stress fields on a local scale. More refined experiments are anticipated when additional information on the actual distribution of rocks at depth, fracture distributions and temperatures become available.

Theoretical variations of stress as a function of depth have as yet been incompletely studied. It can, however, be stated that the horizontal stresses approach the vertical (overburden) stress with increasing depth, as  $T$  approaches  $T_p$ . Near the ground surface, rock temperatures approach a uniform value, and thermoelastic stresses will tend to vanish unless residual stresses reflecting the thermal stress history have previously been 'locked' into the rock mass. This possibility seems a reasonable one, as discussed subsequently.

## Discussion

### *Interpretation of Stresses in the Reykjavik Area*

Though the effects of other sources of stress have not been sufficiently analyzed to completely evaluate their significance, comparison of measured with predicted stresses suggests the possibility that the shallow-crust lateral stress field of the Reykjavik area could be dominantly thermoelastic in origin. A complex regional stress pattern is envisaged, inasmuch as the boundary of the thermal area very nearly abuts against the edge of an active portion of the axial rift zone, where trajectories of minimum compression are perpendicular to dip-slip fault and fissure traces and are consistently NW-trending (Fig. 9).

In the paper by Haimson and Voight (1977, pp. 173–183), it was noted that the Reykjavik measurements indicated maximum horizontal compression (i.e.,  $\sigma_{Hmax}$ , not necessarily  $\sigma_1$ ) roughly normal to the trend of the Reykjanes-Langiökull axial rift zone. This suggested the appropriateness of interpretation in regional terms. Indeed, a new series of stress measurements conducted in 1978 tend to support the concept of systematic reorientation of stress outside rift flanks and  $\sigma_{Hmax}$  realignment roughly normal to the plate boundary (Voight, 1979). But the finite element model results suggest that the two Reykjavik measurement boreholes could have been, by the vicissitudes of fortune, located in areas

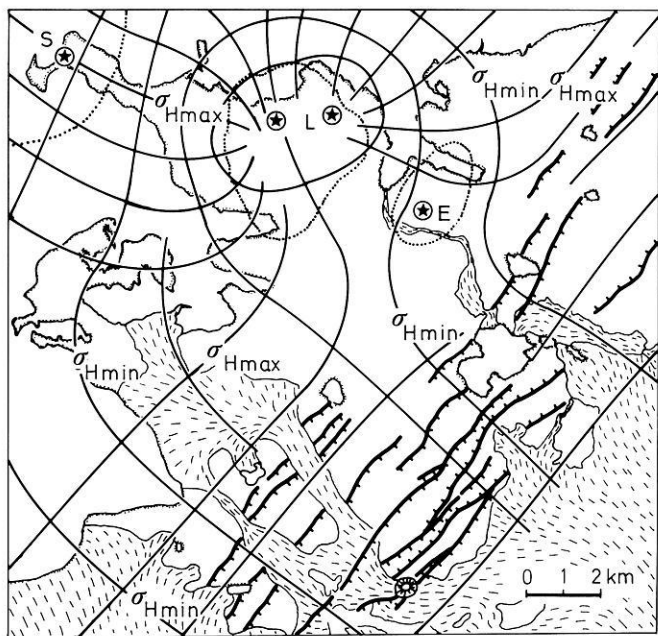


**Fig. 9.** Inferred regional horizontal stress distribution of Reykjavik and adjacent parts of the axial rift zone, southwest Iceland, partly based on models II and III, and extended to encompass the nearby en-echelon fault zone forming part of the Reykjanes-Langjökull axial rift zone (cf. Fig. 1; Haimson and Voight, 1977, Fig. 2). Stippled line at land-sea boundary. Dashed pattern: post-glacial lavas. Circular pattern in the fault zone: a post-glacial volcano. Heavy lines with barbs: faults. Stars: approximate centers of thermal areas. Dotted lines: compression-tensional boundaries according to Model II. S: Seltjarnarnes, L: Laugarnes; E: Ellidaár

characterized by northwest-trending  $\sigma_{Hmax}$  trajectories. Surrounding these sites the stress patterns could be quite different (Figs. 4 and 9). For example, certain boreholes in the vicinity of the Laugarnes thermal area are located in areas of predicted local northeast-trending  $\sigma_{Hmax}$  trajectories. These boreholes, or others appropriately located, could be used for hydrofracturing stress measurements designed to test the merits of competing hypotheses.

The model could also be further tested by fracture orientation measurements in boreholes stimulated for the purpose of increased productivity. Inflatable open hole injection packers have been used for drill hole stimulation in Iceland since 1967, to depths of 2 km (Tómasson and Thorsteinsson, 1975). Predicted fracture orientations are given by Fig. 6. This diagram, considered together with Figs. 4 and 5, could be useful in designing borehole stimulation programs and in examining the possibility of anisotropic hydraulic conductivity associated with thermally induced rock fracture.

Fracturing should be most intense in areas of high tensile and shear stress at the boundary of (or between) high temperature areas. According to Model III, the most severe fracturing should occur between the Laugarnes and Seltjarnarnes thermal areas, in a relatively narrow belt characterized by high tensile (Fig. 4) and high shear stress (Fig. 5). The predicted orientation of extension fractures is given by Fig. 6, although it is recognised that local shear fracturing may also occur depending upon the specifics of the stress state. Well tests in this area could reflect relatively high fracture permeability, unless the fractures have been rather completely mineralized.

Some, and perhaps widespread, mineralization of thermally-induced fractures seems likely. The mineralization provides a mechanism for 'locking in' components of the strain system, and hence the stress system, acting within the rock mass at the time of mineralization. These strains, or more precisely a significant portion thereof, would remain in the rock mass even if it underwent profound temperature changes. Mineralization simply prevents the fractures from closing once the thermal loading is removed; residual strains and associated stresses can thus be locked within the system (cf. Voight, 1974; Friedman, 1972).

According to this view, old thermal areas may still contain residual stress systems which reflect paleotemperature patterns. Such paleotemperature-caused paleostress patterns may also occur in existing thermal areas, inasmuch as temperature changes have been profound in many parts of such systems. In the Reykjavik area, for example, over 1 km of overburden has been removed, and rock now at the ground surface was at one time characterized by a greatly elevated temperature. The near-surface rock mass may still contain residual stresses on the order of  $10^2$  bar which reflect paleotemperature conditions. Indeed, it is not yet possible to state the degree to which the subsurface rocks of the Reykjavik area reflect stress patterns due to the present thermal state, as contrasted to residual stresses associated with previous thermal states.

#### *Thermoelastic Effects in 'Oceanic' Lithosphere*

Thermoelastic effects within the lithosphere are asserted to occur on several scales; they may be subdivided into several 'kinds' according to the scales on which they operate and the general effects which they produce. The resulting regional stress fields are complex inasmuch as they are influenced by superposition.

Stress due to regional cooling of lithospheric plates (as the plates move away from the axial zone of accretion) includes tension roughly parallel to the axial rift zones. These stresses in turn lead to, or influence, the initiation and propagation of fracture zones and transform faults. Such fractures pass *between* local, smaller-scale thermal areas characterized by locally-high thermally-induced compression as indicated by this paper. Mineralization of fractures could cause residual stresses (strains) on the order of  $10^2$  bar to be 'locked' into the rocks in the vicinity of these thermal areas. These residual stresses remain even when the temperatures cool to the regional ambient. Such thermally-induced stresses are likely to be present below the ocean floor, in analogy to their occurrence in Iceland.

Basal lithospheric accretion and cooling, on the other hand, causes components of lateral compression to build up regionally in the upper lithosphere, approximately perpendicular to oceanic crust isochrons. These stresses also are residual but on a different (larger) scale than those associated with thermal anomalies. They build up by gradual thickening and cooling of the oceanic lithosphere as it moves away from a ridge crest. New hot material added to the base of the lithosphere cools with time and places the uppermost part of the plate in compression (Sykes and Sbar, 1974). Beyond some critical isochron such compression may be dominant. But at all locations these stresses would be superimposed upon the residual stress systems associated with the local thermal areas. Local variations in accumulated residual stress components may be considerable and could account for the focal



mechanism "maximum compression direction" discrepancies noted for the basal cooling model by Sykes and Sbar (1974, p. 221).

As a consequence, it seems likely that stresses throughout the upper part of *the entire oceanic lithosphere* may be dominated by superposed patterns of residual (mainly thermal) stress components. If so, it would be incorrect to attribute observed intraplate stresses to plate tectonic forces presently acting on the edges and bases of lithospheric plates, as attempted in recent model studies (e.g., Richardson et al., 1976; Voight et al., 1969). Richardson et al. (1976, p. 1848) recognized a need for some caution in this regard, but concluded that 'there are grounds for believing that the effects of such additional stress-producing mechanisms either are minor or can be minimized by scrutiny of the stress observations chosen to compare against the predictions of force models.' This view is too optimistic with respect to the oceanic lithosphere, if our assessment of the Icelandic data is correct.

*Acknowledgement.* This material is based mainly on work supported by the National Science Foundation under Grant No. EAR 78-12933.

## References

- Friedman, M. Residual elastic strain in rocks. *Tectonophysics* **15**, 297-330, 1972
- Gallagher, R.H. *Finite element Analysis* 420 pp. Englewood Cliffs, NJ: Prentice Hall, 1975
- Haimson, B.C., Voight, B. Crustal stress in Iceland. *Pure Appl. Geophys.* **115**, 153-190, 1977
- Klein, F.W., Einarsson, P., Wyss, M. Microearthquakes on the Mid-Atlantic plate boundary on the Reykjanes Peninsula in Iceland. *J. Geophys. Res.* **78**, 5084-5099, 1973
- Klein, F.W., Einarsson, P., Wyss, M.: The Reykjanes Peninsula, Iceland, earthquake swarm of September 1972 and its tectonic significance. *J. Geophys. Res.* **82**, 865-888, 1977
- Pálmason, G. Geophysical methods in geothermal exploration. Proc. 2nd U.N. Symp. Develop. Use Geothermal Resources 1975

- Pálmason, G., Saemundsson, K. Iceland in relation to the Mid-Atlantic Ridge. *Annu. Rev. Earth Planet. Sci.* **2**, 25-50, 1974
- Richardson, R.M., Solomon, S.C., Sleep, N.H.: Intraplate stress as an indicator of plate tectonic driving forces. *J. Geophys. Res.* **81**, 1847-1856, 1976
- Su, Y.L., Wang, Y.J., Stefanko, R. Finite element analysis of underground stresses utilizing stochastically simulated material properties. Proc. 11th Symp. Rock. Mech., Soc. Min. Engrs., N.Y pp. 253-266, 1970
- Sykes, L.R., Sbar, M.L. Focal mechanism solutions of intraplate earthquakes and stresses in lithosphere. In: *Geodynamics of Iceland and North Atlantic Area*. L. Kristjansson ed. pp. 207-227. Dordrecht. Reidel, 1974
- Tómasson, J., Fridleifsson, I.B., Stefansson, V. A hydrologic model of the flow of thermal water in SW Iceland with a special reference to Reykir and Reykjavik thermal areas. Proc. 2nd U.N. Symp. Develop. Use Geothermal Resources 1975
- Tómasson, J., Thorsteinsson, T Use of injection packer for hydrothermal drillhole stimulation in Iceland. Proc. 2nd U.N. Symp. Develop. Use Geothermal Resources 1975
- Turcotte, D.L. Are transform faults thermal contraction cracks? *J. Geophys. Res.* **79**, 2573-2677, 1974
- Voight, B. A mechanism of 'locking-in' orogenic stress. *Am. J. Sci.* **274**, 662-665, 1974
- Voight, B. Structure and stress history of new hydrofracturing stress measurement sites near the 'mid-ocean' plate boundary in Iceland. *EOS Trans. Am. Geophys. Union*, **60**, 1979
- Voight, B., Samuelson, A.C.. On the application of finite-element techniques to problems concerning potential distribution and stress analysis in the earth sciences. *Pure Appl. Geophys.* **76**, 40-55, 1969
- Voight, B., St. Pierre, H.P.B. Stress history and rock stress. Denver Proc. 3rd Congress, Int. Soc. Rock Mech. 1974
- Voight, B., Taylor, J.W., Voight, J.P. Tectonophysical implications of rock stress measurements. *Geol. Rundsch.* **58**, 655-676, 1969

Received April 30, 1979; Accepted August 10, 1979

## Note Added in Proof

Stress measurements at a Hvalfjörður site 20 km north of Reykjavik suggest a NNW direction of  $\gamma\sigma_{H_{max}}$  (see Haimson, B.C. *EOS Trans. Am. Geophys. Union* 60, 1979).